Influence of Salt on the Self-Assembly of Two Model Amyloid Heptapeptides

V. Castelletto* and I.W. Hamley†

Department of Chemistry, The University of Reading, Reading RG6 6AD, U.K.

C. Cenker and U. Olsson

Physical Chemistry 1, Lund University, S-221 00 Lund, Sweden

Received: March 26, 2010; Revised Manuscript Received: May 10, 2010

We study the effects of NaCl on the self-assembly of AAKLVFF and βAβAKLVFF in solution. Both AAKLVFF and βAβAKLVFF self-assemble into twisted fibers in aqueous solution. The addition of NaCl to aqueous solutions of AAKLVFF produces large crystal-like nanotapes which eventually precipitate. In contrast, highly twisted fibrils were observed for βAβAKLVFF solutions at low salt concentration, while a coexistence of highly twisted fibers and nanotubes was observed for βAβAKLVFF at high salt concentration. The self-assembled structures observed for βAβAKLVFF in NaCl solutions were ascribed to the progressive screening of the βAβAKLVFF surface charge caused by the addition of salt.

1. Introduction

The amyloid β peptide is implicated in amyloid diseases such as Alzheimer's.[1] Fragment KLVFF has been identified as a key sequence involved in β-sheet fibril formation and has been targeted for oligomer-disruption therapies.[2,3] We have recently studied the self-assembly of the extended variant NH_2-Ala-Ala-Lys-Leu-Val-Phe-Phe-COOH (AAKLVFF).[4−7] We focused on the influence of solvent on AAKLVFF, comparing self-assembly in water and methanol and mixtures of these two solvents with different polarities and hydrogen-bonding capacities. We found that in water, AAKLVFF self-assembles into twisted β-sheets,[4] while in methanol, the peptide forms closed nanotubes built out of wrapped β-sheets.[6−8]

Oligomeric peptides containing β-amino acids can self-assemble into helical structures in certain solvents.[9−11] Peptides containing β-amino acids are also of interest in terms of bioactivity, including resistance to proteolysis,[12] also conferring antibacterial[13] or antifungal[14] properties. We have already reported on the aqueous self-assembly of NH_2-β^2Ala-β^2Ala-Lys-Leu-Val-Phe-Phe-COOH (βAβAKLVFF), which is modified at the N terminus with two β^2-alanine residues.[15] We showed that this peptide self-assembles into helical ribbon nanostructures.

Both AAKLVFF and βAβAKLVFF present a positively charged NH_2 group at the N-terminus and a negatively charged COOH group at the C-terminus. It is also expected that the lysine residues in AAKLVFF and βAβAKLVFF are positively charged at a pH lower than 9.59. Despite having similar amino acid sequences and charges, βAβAKLVFF proved to be more water-soluble than AAKLVFF.[4,15]

The two peptides AAKLVFF and βAβAKLVFF can be considered as model systems to investigate charge screening effects on self-assembly and peptide solubility. The effect of salt on solutions of charged self-assembling peptides has been widely studied in the literature. It was found that the addition of NaCl to solutions of the ionic peptide EAK 16-II can influence the dimension of the self-assembled nanostructures.[16] It has been shown that a critical concentration of counterions is needed to allow self-assembly of the charged oligopeptide KFE12 in solution, while KFE12 forms gels only when neutralized.[17] Salt effects also favor gelation at physiological conditions of a series of 11 residue charged peptides, allowing for the development of injectable peptide lubricants for therapeutics.[18] It is known that the presence of salt in the solution triggers the folding process of β-hairpin peptide chains and leads to their self-assembly into hydrogel networks.[19]

The effect of adding salt to solutions containing filamentous proteins involved in neurogenerative diseases has also been investigated. It has been found that the addition of NaCl to solutions of fibrillar aggregates formed from α-synuclein reduces the peptide aggregation time and leads to the formation of amorphous aggregates.[20]

Here, we report the effects of salt (NaCl) concentration on the self-assembly of AAKLVFF and βAβAKLVFF in aqueous solution. This work represents a development of previous work on the self-assembly of AAKLVFF and βAβAKLVFF in water.[4−6,15] Our studies reveal that, upon the addition of NaCl to the solution, AAKLVFF fibers precipitate in fibrous/crystalline nanotapes. In contrast, the addition of NaCl to βAβAKLVFF fibrils enhances the fiber twisting and leads to the coexistence of nanotubes with twisted fibers. The structure of the AAKLVFF and βAβAKLVFF self-assembled aggregates was examined by transmission electron microscopy (TEM) and cryo-TEM. The secondary structure of the peptide fibers and nanotubes was studied by Fourier transform infrared (FTIR) spectroscopy, Raman spectroscopy, circular dichroism (CD), and X-ray diffraction (XRD).

2. Experimental Section

Materials. AAKLVFF (M_w found 795.4) and βAβAKLVFF (M_w found 795.27) were custom-synthesized by C.S. Bio Company (U.S.A.) and were used as received, without further purification. Solutions were made by mixing amounts of peptide in Millipore filtered pure water or solutions containing 50 mM NaCl, 100 mM NaCl, or 250 mM NaCl. The solutions were mixed and left to rest at least for the following hour before collecting experimental data.

* To whom correspondence should be addressed. Tel: 44 118 378 4746. Fax: 44 118 378 6331. E-mail: V.Castelletto@reading.ac.uk.

† Also at Diamond Light Source, Chilton, Didcot, Oxfordshire OX11 0DE, U.K.

10.1021/jp102744g
Published on Web 05/24/2010

TABLE 1: Sample Composition, Salt Concentration, and pH Measured for the Solutions Studied in This Work

sample	mM NaCl	pH
0.5 wt % AAKLVFF	0−250	3.3
1 wt % AAKLVFF	0−300	3→2.4
0.5 wt % βAβAKLVFF	0−250	3
1 wt % βAβAKLVFF	0−250	2.7
1.4 wt % βAβAKLVFF	0−250	2.6

The pH of the solutions studied in this work was measured and is listed in Table 1. It was found that in general, the pH does not vary strongly with the NaCl concentration. The exception was 1 wt % AAKLVFF, for which the pH decreased noticeably when the NaCl concentration increased from 0 to 300 mM. According to Table 1, the solutions are acidic in pure water. As already mentioned in the Introduction, it is expected that the lysine residue has a positive charge in AAKLVFF and βAβAKLVFF aqueous solutions, while the N-terminus has a positive charge and the C-terminus has a negative charge.

Cryo-TEM. Experiments were performed using a Philips CM 120 Bio-Twin transmission electron microscope at Lund University (Lund, Sweden) or a Jeol 2100 microscope at Unilever Corporate Research (Colworth, U.K.). At Lund University, a small quantity of sample was placed on a copper grid in a thermostatted chamber at 25 °C. The sample in the grid was then blotted to create a thin film. At Unilever, the sample was placed on a holey carbon 400 mesh Cu TEM grid in a controlled humidity ([85 ± 3] % RH) chamber at (22 ± 2) °C. The sample on the grid was then blotted using a Gatan Cp3 cryoplunge system to create a thin film.

Both at Unilever and Lund, after blotting, the grid with the sample was quickly vitrified by immersion in liquid ethane[21] and carefully transferred under a liquid nitrogen environment to the microscope. Cryo-TEM was used to characterize samples containing 1−1.4 wt % peptide dissolved in water or aqueous NaCl solutions.

Circular Dichroism. CD spectra were recorded on a Chirascan spectropolarimeter (Applied Photophysics, U.K.). Solutions containing 0.5 wt % peptide, with different amounts of added salt (pure water, 50 mM NaCl, 100 mM NaCl, or 250 mM NaCl), were loaded into a 0.1 mm quartz cells. Spectra were obtained from 200 to 260 nm with a 0.5 nm step and 1 s collection time per step at 20 °C, taking five averages.

FTIR Spectroscopy. Spectra were recorded using a Nexus-FTIR spectrometer equipped with a DTGS detector. Samples containing 1 wt % βAβAKLVFF in different solutions (water or 50−250 mM NaCl) were studied by transmission FT-IR. Small aliquots of peptide solutions were sandwiched between two CaF_2 plate windows (spacer 0.004 mm). Spectra were scanned 128 times.

Rheology. Rheological properties were determined using a controlled stress TA Instruments AR-2000 rheometer (TA Instruments). The viscosity of the samples was measured by performing controlled stress experiments with a cone-and-plate geometry (cone radius = 20 cm; cone angle = 1°). Experiments were performed on samples containing 1 wt % βAβAKLVFF dissolved in water or in NaCl solutions.

Raman Spectroscopy. Raman spectra were recorded using a Renishaw inVia Raman microscope. The light source was a multiline laser, and the experiments were performed using the $\lambda = 785$ nm edge. Experiments were made on stalks prepared by drying filaments of the peptide obtained from βAβAKLVFF dissolved in water or NaCl solutions. The stalks were focused by using a ×20 magnification lens. Spectra were obtained in the interval of 100−3000 cm^{-1}, using a collection time of 20 s, with a 10% laser power and by taking two averages.

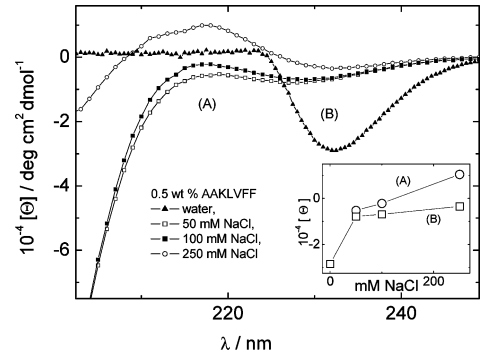

Figure 1. CD data for 0.5 wt % AAKLVFF solutions in pure water, 50 mM NaCl, 100 mM NaCl, and 250 mM NaCl. The inset shows the dependence of the molar ellipticity in regions (A) and (B) on the concentration of NaCl.

XRD. X-ray diffraction was performed on the same stalks as those used for Raman experiments. The stalks were mounted (vertically) onto the four axis goniometer of a RAXIS IV++ X-ray diffractometer (Rigaku) equipped with a rotating anode generator. The XRD data were collected using a Saturn 992 CCD camera.

3. Results and Discussion

The secondary structure of AAKLVFF in water and in NaCl solutions was assessed by CD experiments. The corresponding results are presented in Figure 1. The CD data for the sample in pure water in Figure 1 are extracted from our previous work on AAKLVFF[4] and are displayed as a reference. The CD spectra in Figure 1 are dominated by a maximum at ∼218 nm and a minimum at ∼232 nm. A prominent single maximum at ∼220 nm and a minimum at 230 nm have been previously reported by us in the CD spectrum for aqueous solutions of βAβAKLVFF,[15] AAKLVFF,[4] or FFKLVFF.[22] A strong positive band at 218 nm in the CD spectra (Figure 1) results from the π−π* interactions of the amide groups.[23] The broad negative band near 225 nm in the CD spectra (Figure 1) is associated with the n−π* transition of the amide groups.[23] Indeed, the features of the CD data in Figure 1 point to peptides in which self-assembly into structures lacking defined secondary structure is driven by aromatic interactions of phenylalanine units.[24]

The inset in Figure 1a shows the ellipticity values at ∼218 (region A) and ∼232 nm (region B) as a function of the NaCl content. Only the ellipticity at 218 nm increases simultaneously with NaCl concentration. It is possible that charge screening effects reduce repulsion between lysine units and thus indirectly enhance phenylalanine aromatic screening interactions.

The self-assembly of AAKLVFF was further studied by cryo-TEM. Figure 2 shows images obtained for 1 wt % AAKLVFF in water, with 100 and 300 mM NaCl. While 1 wt % AAKLVFF aqueous solutions were transparent to the naked eye, samples containing NaCl and 1 wt % peptide were cloudy. The latter samples showed, after a few days of incubation, a milky portion of the solution separated at the bottom of the flask, coexisting with a transparent portion of the solution at the top of the flask. Cryo-TEM experiments for NaCl solutions in Figure 2 were made on freshly made cloudy solutions.

The Cryo-TEM image in Figure 2a for 1 wt % AAKLVFF has previously been published by us.[6] It contains individual fibrils or bundles of 2−3 fibers twisted around the main fibril axis. The individual fibrils are (18.5 ± 3.3) nm thick and more

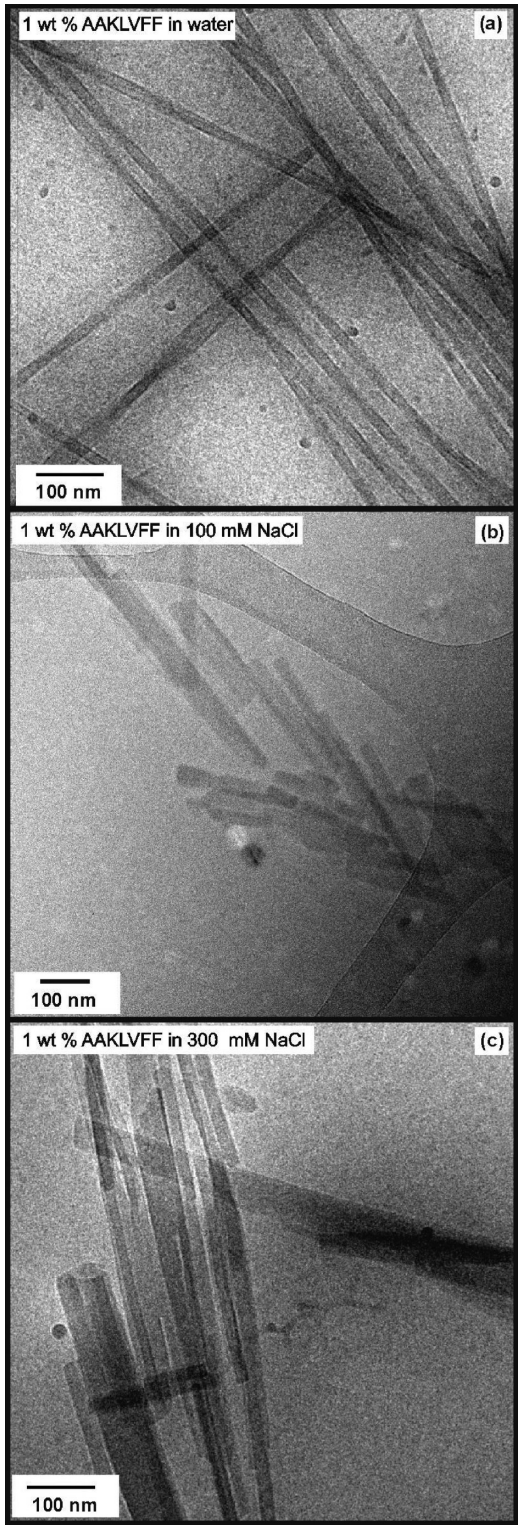

Figure 2. Cryo-TEM images obtained for 1 wt % AAKLVFF solutions dissolved in (a) water, (b) 100 mM NaCl, and (d) 300 mM NaCl.

than 4 μm long. Figure 2b,c shows the formation of rigid tapes with a crystal-like shape for 1 wt % AAKLVFF in 100−300 mM NaCl. Individual tapes are (22.4 ± 2.3) nm thick, but they can be joined together in thicker tapes that are (124.7 ± 6.9) nm thick.

The aggregates shown in Figure 2b,c are responsible for the cloudiness of fresh AAKLVFF solutions containing NaCl and their subsequent precipitation after a few days of incubation.

Fraser and co-workers reported aggregation of fibrils into tapes for peptide Aβ(11−28), which contains the KLVFF motif

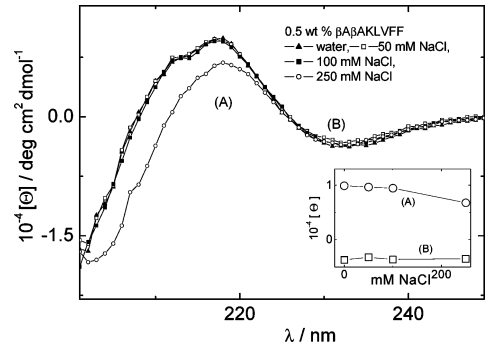

Figure 3. CD data for 0.5 wt % βAβAKLVFF solutions in water, 50 mM NaCl, 100 mM NaCl, and 250 mM NaCl. The inset shows the dependence of the molar ellipcity in zones (A) and (B) on the concentration of NaCl.

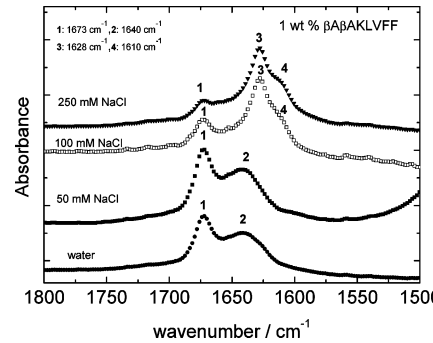

Figure 4. FTIR data for 1 wt % βAβAKLVFF solutions in water, 50 mM NaCl, 100 mM NaCl, and 250 mM NaCl.

Aβ(16−20) within AAKLVFF.[25] It was shown that addition of 100 mM NaCl to solutions of Aβ(11−28) led to the lateral aggregation of three to five fibrils into ∼50 nm thick tapes. In addition, comparable conditions with a sulfate salt caused Aβ(11−28) to undergo an extensive lateral aggregation into ∼150 nm thick tapes.

A variation of the heptapeptide sequence might be an alternative path to stabilize AAKLVFF solutions against charge screening effects. We then decided to study charge screening effects on βAβAKLVFF since this peptide proved to be more soluble in water than AAKLVFF. Charge screening effects were then studied in βAβAKLVFF solutions in water or 50−250 mM NaCl. Higher NaCl concentrations solutions were also prepared, but they produced weakly cloudy samples, which were not studied further.

The secondary structure of the βAβAKLVFF in solutions with varying salt concentration was first assessed by CD. Figure 3 shows spectra obtained for samples containing 0.5 wt % βAβAKLVFF in water and 50−250 mM NaCl. The CD spectra in Figure 3 are dominated by a maximum at ∼218 nm and a minimum at ∼232 nm, already discussed in relation to the CD results in Figure 1. In contrast to the spectra for AAKLVFF (Figure 1), the ellipticities at 218 and 232 nm do not change appreciably with NaCl concentration.

The secondary structure of the self-assembled peptide in solution was also studied by transmission FTIR. Figure 4 shows the Amide I and Amide II regions of the FTIR spectra measured for D_2O solutions of 1 wt % βAβAKLVFF in water and 50−250 mM NaCl.

All of the FTIR spectra shown in Figure 4 present a peak at 1673 cm^{-1}, which corresponds to the contribution of the TFA to the FTIR spectra since the peptide was provided as a TFA salt by the manufacturer. This peak becomes less important as

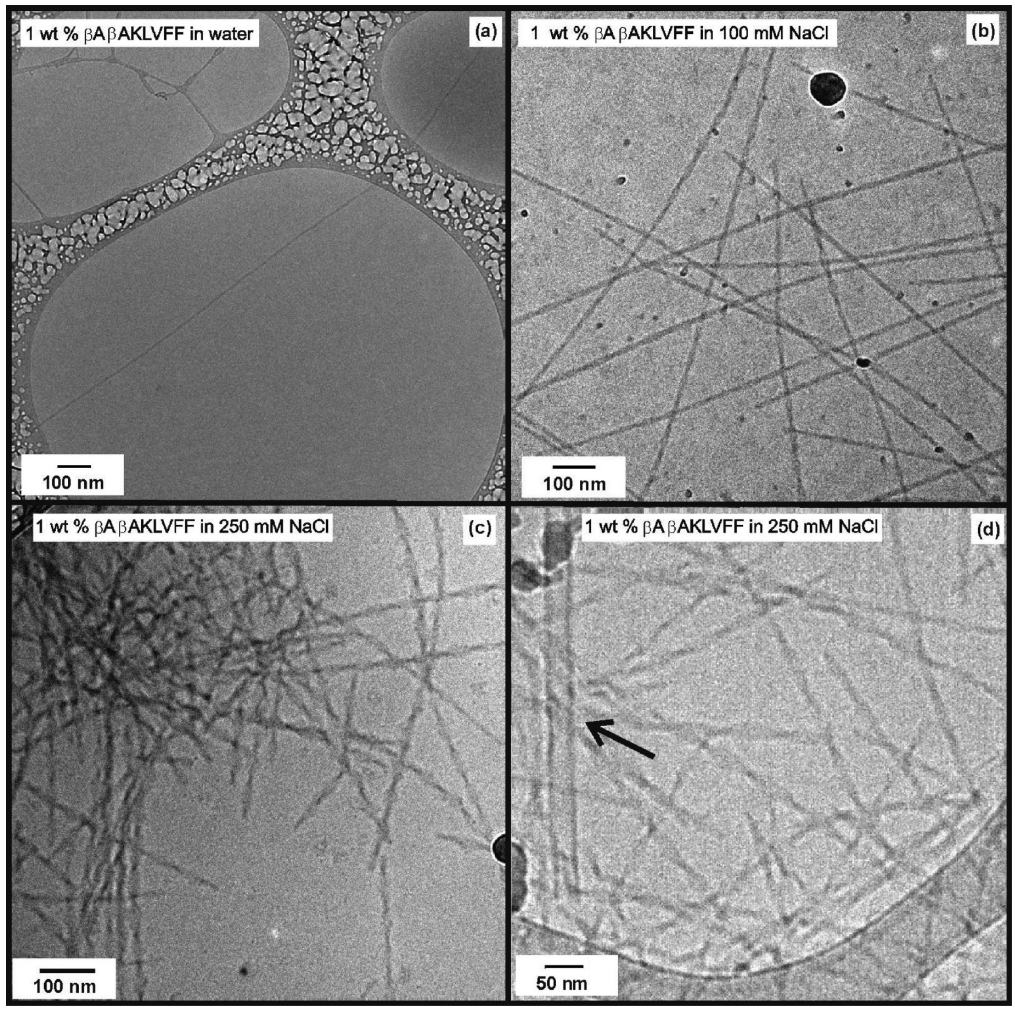

Figure 5. Cryo-TEM images obtained for 1 wt % βAβAKLVFF solutions dissolved in (a) water, (b) 100 mM NaCl, or (c,d) 250 mM NaCl. The arrow points to a nanotube.

the NaCl concentration is increased due to TFA/Cl ion exchange. FTIR spectra also show peaks centered at 1628 and 1640 cm^{-1} (Figure 4). The peak at 1628 cm^{-1} is associated with a β-sheet structure.[26,27] The peak at 1640 cm^{-1} may either be a frequency-shifted β-sheet peak or due to random coil secondary structure.[27]

It is interesting to notice that only samples containing 100 mM NaCl and 250 mM NaCl present a FTIR peak at 1610 cm^{-1}. FTIR peaks at around 1605−1610 cm^{-1} have been observed in the spectra of ^{13}C isotopically labeled peptides forming β-sheets[28−30] and some peptides containing sequences found in βAβAKLVFF, such as KLVFFAE[31] or peptides containing sequences of K, L, and A amino acids.[32] However, the origin of the FTIR peak at 1610 cm^{-1} in Figure 4 is not clear since there is no reason to expect effects related to isotope enrichment. It could be related to the exchange of residual trifluoroacetate (TFA) for Cl counterions, which might increase the "effective mass" of one of the residues (e.g., lysine or the N-terminus with which the counterion is associated).

According to our previous studies,[15] βAβAKLVFF self-assembles into helical β-sheet ribbons in water, at concentrations similar to those studied in Figure 4. The FTIR results show a β-sheet structure, although additional random coil secondary structure might be present for pure water and 50 mM NaCl.

In light of these results, it is interesting to directly assess the possible existence for β-sheets and random coil structures resulting from the self-assembly of βAβAKLVFF in solution. Evidence for self-assembly in solution is provided by cryo-TEM. Figure 5 shows cryo-TEM images obtained for 1 wt % βAβAKLVFF in water and 100 and 250 mM NaCl.

Figure 5a shows that 1 wt % βAβAKLVFF in water produces flexible fibers that are (8.7 ± 1.1) nm thick. It should be mentioned that the 1 wt % βAβAKLVFF tapes in Figures 5a are not as twisted as the helical nanoribbons reported by us in our previous work for 2 wt % βAβAKLVFF.[15] We ascribe this difference to a concentration effect.

In a 100 mM NaCl solution (Figure 5b), twisted tapes are observed which are (11.9 ± 1.4) nm thick with a (61.3 ± 7.6) nm long pitch. Peptide fibrils observed for 250 mM NaCl are very similar to those observed for 100 mM NaCl, having a (10.2 ± 2.0) nm thickness and (61.1 ± 10.5) nm pitch (Figure 5c). Figure 5c shows the extent of fibril twisting upon increasing the NaCl concentration from 100 to 250 mM NaCl. Figure 5d also shows the formation of a fraction of nanotubes for 1 wt % βAβAKLVFF in 250 mM NaCl. These nanotubes are (31.4 ± 0.8) nm broad with (3.9 ± 0.7) nm thick walls. Figures 5 indicates self-assembly of βAβAKLVFF into β-sheets. Although additional random coil secondary structure (detected by FTIR) might be present, it does not disrupt the nanotube or fibril formation.

The twisting enhancement of the fibrils and the formation of nanotubes at 250 mM NaCl might be due to screening of charge on the edge of the peptide fibrils. A possible mechanism for the twisting of the fibrils and the formation of nanotubes as a consequence of charge screening effects is depicted in Scheme

SCHEME 1: Mechanism for (a) Fiber Twisting or (b) Nanotube Formation Upon Screening the Surface Charge on *β*A*β*AKLVFF *β*-Sheets[a]

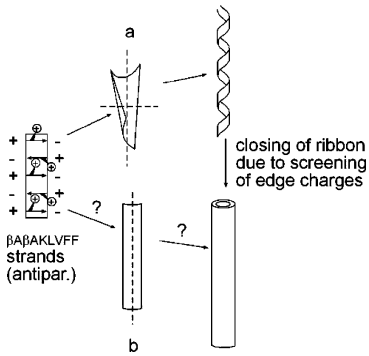

[a] The charged lysine residue gives rise to off-axis charge (and dipole) shown as ⊕.

1. At a molecular level, self-assembly is driven by a combination of hydrogen bonding within the β-sheet and hydrophobic and electrostatic interactions of the side chains between β-sheets. The β-strands in βAβAKLVFF appear to have an antiparallel arrangement to give zero net charge and dipole, considering the charged termini alone (Scheme 1). In pure water, the lysine residue is charged, and the charge is off the strand axis, giving rise to a net charge (Scheme 1). The addition of NaCl to βAβAKLVFF aqueous solutions partially screens the β-sheet surface charge. This allows the fibrils, at low NaCl concentrations, to adopt a twisted structure (path (a) in Scheme 1). However, if the energy barrier of the electrostatic repulsion is sufficiently decreased, at high NaCl concentrations, the charge on the ribbon edges can be screened. In this way, the β-strands self-assemble into a nanotube formed by wrapped β-sheets (path (b) in Scheme 1).

However, it is not a general rule that a fibril-to-nanotube transition is observed upon charge screening upon NaCl addition in solutions containing charged peptide fibrils. For example, the presence of 25 mM NaCl was found to increase the compactness of amyloid fibers from the SH3 domain of the α-subunit of bovine phosphatidylinositol-3′-kinase (PI3-SH3).[33] Similarly to PI3-SH3, the filamentous protein α-synuclein forms charged fibrillar aggregates upon incubation under physiological conditions.[20] However, addition of 200 mM NaCl reduces the fibrillization rate and favors the formation of large, amorphous aggregates.

In addition, the opposite behavior to that found in Figure 5 (i.e., nanotube−fibril transition driven by the addition of NaCl to the solution) has been reported in the literature. Peptide−dendron hybrids self-assemble into charged nanotubes in water.[34] It has been shown that increasing the NaCl concentration from 0 to 100 mM results in the transformation of nanotubes into fibrils for salt concentrations higher than 50 mM NaCl.

The viscosity of the βAβAKLVFF samples was investigated by rheology. Figure 6 shows the viscosity data obtained for 1 wt % βAβAKLVFF in water, 50 mM NaCl, 100 mM NaCl and 250 mM NaCl. The viscosity of the samples increases steadily with the NaCl concentration (inset Figure 6).

The cryo-TEM images in Figure 5 show that the thickness of βAβAKLVFF fibrils does not change with NaCl concentration, but it does suggest increased fibril bundling (and a decrease in persistence length) with increasing salt concentration. Additional information about this can be deduced from Figure 6 since the increase in viscosity with NaCl concentration might arise from enhanced interactions between peptide fibrils at higher

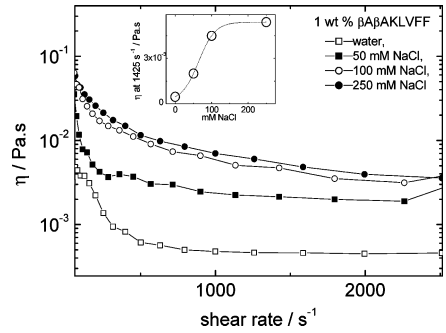

Figure 6. Viscosity η measured for 1 wt % βAβAKLVFF solutions in water, 50 mM NaCl, 100 mM NaCl, and 250 mM NaCl. The inset shows the dependence of η (averaged over values at 1140 and 2250 s^{-1}) on the NaCl concentration.

NaCl concentration, where surface charge is screened. In addition, there is an additional contribution to the viscosity from the coexistence of nanotubes with fibrils in 250 mM NaCl.

An increase in the elastic modulus (and, consequently, the viscosity of the material) of β-hairpin peptides upon addition of NaCl to the solution has been previously reported. Intramolecular folding is triggered by the addition of NaCl to solutions of β-hairpin peptides.[19] Without salt, the electrostatic repulsion of the lysine residues in the β-hairpin peptides keeps the peptides unfolded, frustrating self-assembly. The addition of NaCl folds the molecule, allowing for intermolecular hydrophobic interactions and hydrogen bond formation. The β-hairpin molecules are interconnected in a fibrillar network in the presence of salt. Increasing the NaCl concentration increases the number of junction points in the interconnected network and consequently increases the elastic modulus of the material.

However, there are no branch points between the fibers or nanotubes in the cryo-TEM images displayed in Figure 5, making more feasible the possibility that the increase in viscosity upon adding NaCl (Figure 6) arises from interactions between overlapping fibrils (with screened surface charge). This differs from an increase in fibril persistence length observed for amyloid fibrils formed by other proteins and peptides. The effect of electrostatic interactions on the percolation concentration (obtained from controlled strain rheometry) was studied for charged β-lactoglobulin fibers at pH 2.[35] The results obtained for several β-lactoglobulin solutions, with salt content in the range of 20−200 mM NaCl, indicated that screening of the surface charge on fibrils weakens repulsive electrostatic interactions and allows for fibril extension. The effect of NaCl on the self-assembly of solutions of the ionic complementary peptide EAK16-II has been investigated.[16] It has been found that the presence of NaCl does not significantly influence the critical aggregation concentration of the peptide. A critical salt concentration was also observed, below which the average peptide fibril dimensions increased with salt concentration but above which the opposite behavior was noted.

Charge repulsion has also been predicted to be the primary force preventing the growth of fibers of the charged peptide $K_2(QL)_6K_2$.[36] The addition of 150 mM NaCl to a solution of $K_2(QL)_6K_2$ fibrils led to an increase in the fibril length, although the solution did not gel. Gelation was obtained upon addition of 1 M NaCl, which dramatically increased the length of the fibrils such that a sample-spanning network was obtained.

We have shown in our previous study of βAβAKLVFF[15] and AAKLVFF[4,6] that there is a correspondence between structures observed for solutions in situ (via cryo-TEM) and those from negative stain TEM for dried samples. Therefore, we further

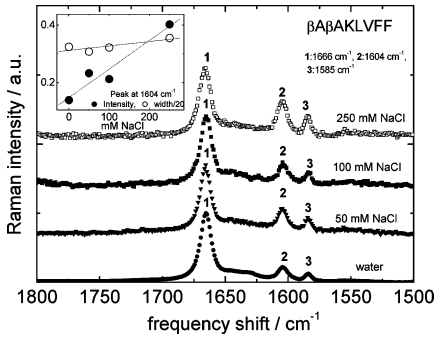

Figure 7. Raman spectra (shown with arbitrary offset for clairity) for dried stalks prepared from solutions containing 6 wt % βAβAKLVFF in water or 1 wt % βAβAKLVFF in 50 mM NaCl, 100 mM NaCl, or 250 mM NaCl. The inset shows the dependence of the height and the width of the peak at 1604 cm^{-1} on the NaCl concentration in the sample.

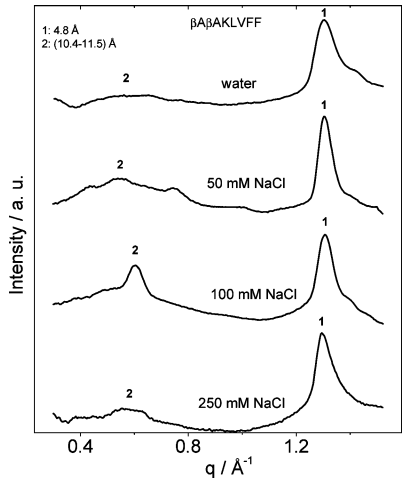

Figure 8. XRD spectra for dried stalks prepared from solutions containing 6 wt % βAβAKLVFF in water or 1 wt % βAβAKLVFF in 50 mM NaCl, 100 mM NaCl, or 250 mM NaCl.

studied the secondary structure by drying stalks of NaCl-containing samples and performing Raman and XRD experiments on them. It was not possible to prepare a stalk for the 1 wt % βAβAKLVFF solution in water used for the FTIR studies (Figure 4) due to its low viscosity, and therefore, a 6 wt % peptide aqueous solution was used instead.

Figure 7 shows the Raman spectra recorded for stalks dried from βAβAKLVFF solutions. All of the Raman spectra in Figure 7 present peaks at 1666, 1604, and 1585 cm^{-1}. Peaks at 1666 and 1604 cm^{-1} in Figure 7 are associated with β-sheet structure, in good agreement with FTIR results for the corresponding samples in solution (Figure 4). A Raman band at 1587 cm^{-1} has been assigned to phenylalanine residues in the literature[37] and probably corresponds to the Raman peak measured at 1585 cm^{-1} in Figure 7. The Raman spectra for the dried stalks in Figure 7 do not show any evidence of random coil structure observed for solutions in water or 50 mM NaCl in Figure 4. This is similar to our previous observations for KLVFF[38] and shows that drying enhances β-sheet formation in KLVFF-based peptides. By normalizing the Raman peak intensities, with respect to the intensity of the peak at 1666 cm^{-1}, the intensity and the height of the peak at 1604 cm^{-1} can be seen to increase with the NaCl concentration (inset in Figure 7).

Figure 8 displays the radially averaged XRD data (from 2D patterns) measured for the same dried stalks of βAβAKLVFF used to obtain the Raman results displayed in Figure 7. Reflections at ~4.8 and ~12 Å can be observed in all of the profiles in Figure 8. However, the relative intensity of the peak at ~4.8 Å with respect to the peak at ~12 Å increases upon increasing the NaCl content in the sample. This suggests that the long-range stacking order of the β-sheets (which gives rise to the 12 Å reflection) decreases as the NaCl concentration increases. This might in part result from splay caused by twisting of the β-sheet fibrils.

The influence of the sample concentration was studied for samples at a fixed NaCl concentration (250 mM) using cryo-TEM. Cryo-TEM results obtained for a 1.4 wt % peptide solution show the formation of 6.6 ± 0.9 nm thick fibers with a 130.8 ± 21.5 nm in pitch length (Figure 9a,b). A few nanotubes, 18.2 ± 1.1 nm broad with 2.6 ± 0.3 nm thick walls, coexist with the fibers. There are more nanotubes than in the corresponding cryo-TEM image for 1 wt % peptide at the same salt concentration (Figure 5d).

4. Summary

In this work, we studied the effect of NaCl on the self-assembly of AAKLVFF and βAβAKLVFF in solution. Our results show that, although having a very similar amino acid sequence, both peptides behave in dramatically different ways in the presence of NaCl.

AAKLVFF self-assembles into twisted fibers in aqueous solution. The addition of NaCl to aqueous solutions of this

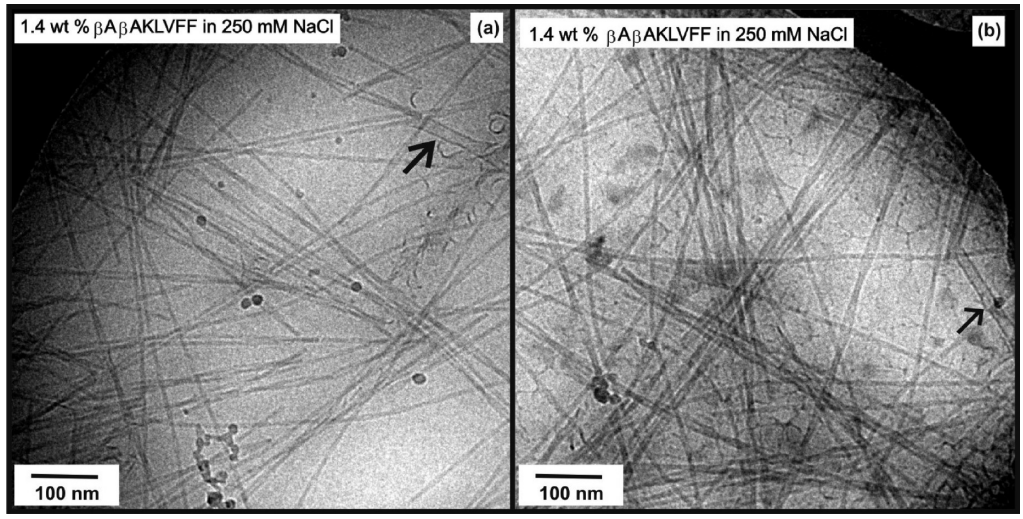

Figure 9. Cryo-TEM images obtained for 1.4 wt % βAβAKLVFF in 250 mM NaCl. The arrows point to short nanotubes.

peptide produces large crystal-like nanotapes which eventually precipitate, showing that salt-induced screening leads to phase separation in this marginally soluble peptide.

In contrast to AAKLVFF, the addition of NaCl to βAβAKLVFF aqueous solutions produced homogeneous transparent solutions. Peptide βAβAKLVFF produced twisted fibers in pure water. Highly twisted peptide fibrils were observed for solutions at low salt concentration, while a coexistence of highly twisted fibers and peptide nanotubes was observed at high salt concentration. The enhancement of the peptide fibril twisting and the formation of nanotubes upon increasing the NaCl concentration were ascribed to the progressive screening of the peptide surface charge caused by the addition of salt to the solution. The observed enhancement in viscosity with increasing salt concentration was ascribed to increased interfibril interactions due to charge screening, leading to dense overlapped fibril bundles. Novel features were observed in the FTIR and Raman spectra at high salt concentration, possibly associated with counterion effects changing the effective mass of specific residues. Finally, changes in the cross-β packing mode were revealed by X-ray diffraction on dried stalks.

Acknowledgment. We thank Dr Rebecca Green (Department of Pharmacy, University of Reading) for access to the FTIR. We are grateful to Mr Nick Spencer (The Biocentre, University of Reading) for his support during the XRD experiments. We are grateful to Steve Furzeland and Derek Atkins (Unilever, Colworth, U.K.) for performing the cryo-TEM experiments.

References and Notes

(1) Hamley, I. W. *Angew. Chem., Int. Ed.* **2007**, *46*, 8128–8147.
(2) Austen, B. M.; Paleologou, K. E.; Ali, S. A. E.; Qureshi, M. M.; Allsop, D.; El-Agnaf, O. M. A. *Biochemistry* **2008**, *47*, 1984–1992.
(3) Doig, A. J. *Curr. Opin. Drug Discovery Dev.* **2007**, *10*, 533–539.
(4) Castelletto, V.; Hamley, I. W.; Harris, P. J. F. *Biophys. Chem.* **2008**, *138*, 29–35.
(5) Hamley, I. W.; Krysmann, M. J. *Langmuir* **2008**, *24*, 8210–8214.
(6) Castelletto, V.; Hamley, I. W.; Harris, P. J. F.; Olsson, U.; Spencer, N. *J. Phys. Chem. B* **2009**, *13*, 9978–9987.
(7) Hamley, I. W.; Nutt, D. R.; Brown, G. D.; Miravet, J. F.; Escuder, B.; Rodriguez-Llansola, F. *J. Phys. Chem. B* **2010**, *114*, 940–951.
(8) Krysmann, M. J.; Castelletto, V.; McKendrick, J. M. E.; Hamley, I. W.; Stain, C.; Harris, P. J. F. *Langmuir* **2008**, *24*, 8158–8162.
(9) Seebach, D.; Overhand, M.; Kuhnle, F. N. M.; Martinoni, B.; Oberer, L.; Hommel, U.; Widmer, W. *Helv. Chim. Acta* **1996**, *79*, 913–941.
(10) Seebach, D.; Matthews, J. L. *Chem. Commun.* **1997**, 2015–2022.
(11) Cheng, R. P.; Gellman, S. H.; DeGrado, W. F. *Chem. Rev.* **2001**, *101*, 3219–3232.
(12) Arvidsson, P. L.; Ryder, N. S.; Weiss, H. M.; Hook, D. F.; Escalante, J.; Seebach, D. *Chem. Biodiversity* **2004**, *2*, 401–420.
(13) Raguse, T. L.; Porter, E. A.; Weisblum, B.; Gellman, S. H. *J. Am. Chem. Soc.* **2002**, *124*, 12774–12785.
(14) Karlsson, A. J.; Pomerantz, W. C.; Weisblum, B.; Gellman, S. H.; Palecek, S. P. *J. Am. Chem. Soc.* **2006**, *128*, 12630–12631.
(15) Castelletto, V.; Hamley, I. W.; Hule, R. A.; Pochan, D. J. *Angew. Chem., Int. Ed.* **2009**, *48*, 2317–2320.
(16) Hong, Y.; Pritzker, M. D.; Legge, R. L.; Chen, L. *Colloids Surf., B* **2005**, *26*, 152–161.
(17) Caplan, M. R.; Moore, P. N.; Zhang, S.; Kamm, R. D.; Lauffenburger, D. A. *Biomacromolecules* **2000**, *1*, 627–631.
(18) Carrick, L. M.; Aggeli, A.; Boden, N.; Fisher, J.; Ingham, E.; Waigh, T. A. *Tetrahedron* **2007**, *63*, 7457–7467.
(19) Ozbas, B.; Kretsinger, J.; Rajagopal, K.; Schneider, J. P.; Pochan, D. J. *Macromolecules* **2004**, *37*, 7331–7337.
(20) Hoyer, W.; Antony, T.; Cherny, D.; Heim, G.; Jovin, G. M.; Subramaniam, V. *J. Mol. Biol.* **2002**, *322*, 383–393.
(21) Talmon, Y. *Ber. Bunsen-Ges. Phys. Chem.* **1996**, *3*, 364–372.
(22) Krysmann, M. J.; Castelletto, V.; Hamley, I. W. *Soft Matter* **2007**, *2*, 1401–1406.
(23) Peggion, E.; Palumbo, M.; Bonora, G. M.; Toniolo, C. *Bioorg. Chem.* **1974**, *3*, 125–132.
(24) Gupta, M.; Bagaria, A.; Mishra, A.; Mathur, P.; Basu, A.; Ramakumar, S.; Chauhan, V. S. *Adv. Mater.* **2007**, *19*, 858.
(25) Fraser, P. E.; Nguyen, J. T.; Chin, D. T.; Kirschner, D. A. *J. Neurochem.* **1992**, *59*, 1531–1540.
(26) Haris, P.; Chapman, D. *Biopolymers* **1995**, *37*, 251–263.
(27) Stuart, B. *Biological Applications of Infrared Spectroscopy*; Wiley: Chichester, U.K., 1997.
(28) Paul, C.; Axelsen, P. H. *J. Am. Chem. Soc.* **2005**, *127*, 5754–5755.
(29) Petty, S. A.; Decatur, S. M. *J. Am. Chem. Soc.* **2005**, *127*, 13488–13489.
(30) Mehta, A. K.; Lu, K.; Childers, W. S.; Liang, Y.; Dublin, S. N.; Dong, J. J.; Snyder, J. P.; Pingali, S. V.; Thiyagarajan, P.; Lynn, D. G. *J. Am. Chem. Soc.* **2008**, *130*, 9829–9835.
(31) Decatur, S. M. *Acc. Chem. Res.* **2006**, *39*, 169–175.
(32) Kubelka, J.; Keiderling, T. A. *J. Am. Chem. Soc.* **2001**, *123*, 6142–6150.
(33) Zurdo, J.; Guijarro, J. I.; Jimenez, J. L.; Saibil, H. R.; Dobson, C. M. *J. Mol. Biol.* **2001**, *311*, 325–340.
(34) Shao, H.; Parquette, J. R. *Angew. Chem., Int. Ed.* **2009**, *48*, 2525–2528.
(35) Veerman, C.; Sagis, L. M. C.; Heck, J.; van der Linden, E. *Int. J. Biol. Macromol.* **2003**, *31*, 139–146.
(36) Dong, H.; Paramonov, S. E.; Aulisa, L.; Bakota, E. L.; Hartgerink, J. D. *J. Am. Chem. Soc.* **2007**, *129*, 12468–12472.
(37) Yu, N. T.; Liu, C. S.; O'Shea, D. C. *J. Mol. Biol.* **1972**, *70*, 117–132.
(38) Krysmann, M. J.; Castelletto, V.; Kelarakis, A.; Hamley, I. W.; Hule, R. A.; Pochan, D. J. *Biochemistry* **2008**, *47*, 4597–4605.

JP102744G